Bidirectional extracellular electron transfers in *Serratia marcescens* and *Stenotrophomonas sp.* correlate to EPS and Cr(VI) removal in single-chamber bioelectrochemical systems

Yiying Yan[a], Qiang Wang[b], Liping Huang[a,*], Xin Xing[a], Yong Shi[a], Miao Wang[c], Gianluca Li Puma[d,*]

[a] Key Laboratory of Industrial Ecology and Environmental Engineering, Ministry of Education (MOE), School of Environmental Science and Technology, Dalian University of Technology, Dalian, 116024, China

[b] Jiangxi Academy of Eco-Environmental Sciences and Planning, Nanchang, 330000, China

[c] School of Life Science and Biotechnology, Dalian University of Technology, Dalian 116024, China

[d] Environmental Nanocatalysis & Photoreaction Engineering, Department of Engineering, University of Palermo (UNIPA), Palermo, 90128, Italy

Short title: *Inward/outward EETs correlate to EPS in single-chamber BESs for Cr(VI) removal*

E-mail address: lipinghuang@dlut.edu.cn (L. Huang).

gianluca.lipuma@unipa.it (G. Li-Puma)

The authors declare no competing financial interest.

Abstract

The electrochemically active bacteria (EAB) *Stenotrophomonas* sp. YS1 and *Serratia marcescens* Q1 with bidirectional extracellular electron transfer (EET) were

investigated for the removal of heavy metals (e.g., Cr(VI)) limited by carbon/electron sources or electron acceptors in single-chamber bioelectrochemical systems (BESs). A range of analytical methods including cyclic voltammetry, differential pulse voltammetry, quantitative extracellular polymeric substances (EPS) analysis and EPS material diversity by fluorescence excitation-emission matrix spectroscopy were used to characterize the process. The biofilms of these Cr(VI)-tolerant EAB exhibited bidirectional EET metabolizing either organic (acetate) or inorganic (HCO_3^-) species with simultaneous removal of Cr(VI). Q1 inward EET uptake of electrons was more efficient than that of YS1 (165 μA vs. 118 μA) while, YS1 outward EET was more efficient than Q1 (8.0 μA vs. 4.7 – 5.2 μA). The adaptive electrochemically-tunable EPS in both biofilms strains was regulated by the direction of the EET (inward or outward) in the presence of Cr(VI) and circuital current. This study demonstrates the switching properties of EAB such as *Stenotrophomonas* sp. or *S. marcescens* capable of bidirectional EET to or from the electrodes and the regulation of such response with the amount and compositional diversity of the biofilms EPS, giving a comprehensive appreciation of such tunable EPS for Cr(VI)-wastewater treatment in single-chamber BESs.

Keywords: bidirectional extracellular electron transfer; extracellular polymeric substances; Cr(VI) removal; electrochemically active bacteria

1 Introduction

Electrochemically active bacteria (EAB) acting as bio-oxidation or bio-reduction catalysts, donating or accepting electrons from redox-active species or electrodes have

47 recently gained increasing attention, particularly for the development of
48 bioelectrochemical systems (BESs) applied for environmental remediation and
49 production of renewable energy (Molenaar et al., 2016; Nguyen et al., 2016; Jiang and
50 Zeng 2019). Such EAB capable of bidirectional extracellular electron transfer (EET)
51 either outward EET (electrons flowing from the interior of EAB towards anodes) or
52 inward EET (electrons flowing from cathodes across the cell membrane into the interior
53 of cells), largely controls the efficiency of interaction and electrical communication
54 between biofilm and electrode and thus BESs system performance (Molenaar et al.,
55 2016; Jiang and Zeng 2019). Recently, it has demonstrated that pure EAB immobilized
56 over cathodes of dual-chamber BESs are capable of inward EET utilizing HCO_3^- or
57 methane with simultaneous removal of heavy metals (e.g., Cr(VI) or Au(II)) (Xue et al.,
58 2017; Dominguez-Benetton et al., 2018; Qian et al., 2019; Huang et al., 2021a; 2021b;
59 Wang et al., 2021). However, the behavior of such metallurgical EAB capable of
60 bidirectional EET has yet to be investigated in single-chamber BESs treating heavy
61 metal-based wastewaters (e.g, from the etching and cleaning processes in the electronic
62 industry) limited by carbon/electron sources or electron acceptors (Jiang and Zeng 2019;
63 Huang et al., 2021b; Huang and Li Puma 2022a). In such processes, one important
64 aspect that needs to be elucidated is the adaptive response of the EAB, through the
65 production of extracellular polymeric substances (EPS), in relation to the direction of
66 the EET (inward or outward) in the presence of Cr(VI) and circuital current. EPS
67 facilitate the adhesion of EAB cells on the electrode surface and reduce the EAB-
68 electrode gap for EET, thus saving the energy needed to reach the reactive species

(acceptors/donors) (Xiao et al., 2017). Moreover, EPS act as transient media harboring *c*-type cytochromes or riboflavin-like mediators in single outward or inward EET processes in the absence of heavy metals (Xiao et al., 2017; Yu, 2020; Huang and Li Puma, 2022). The stronger redox-active exoproteins components of EPS enhance the EPS conductivity and thus the EET, while the EPS exopolysaccharides support cell adhesion and the maintenance of cell envelope integrity and aggregation. Recent studies have shown that heavy metals such as Au(III) or Cr(VI) stimulated *Methylomonas* sp. and *Serratia marcescens* to produce EPS with high redox activity but with a higher faradaic resistance, which as a compromise hindered the inward EET for the metals reduction, (Sun et al., 2021; Wang et al., 2021). This behavior suggests that the electrochemically-tunable EPS species may be used to regulate the bidirectionality of EAB, however, the role of EPS in these switchable EAB with bidirectional EET and in the presence of heavy metals remains unexplored. Understanding the behavior of EPS in bidirectional EET is of vital importance for deepening our knowledge on both the opportunistic EAB with bidirectional EET, and on the strategic interaction between the EAB biofilm and the electrode surface to achieve efficient heavy metals removal in BESs (Huang and Li Puma, 2022). Understanding these aspects could allow the possibility of using tunable EPS to control the activities of EAB and the switchable EET towards the removal/reduction of desired heavy metals from wastewaters containing complex inorganic or/and organic carbons as well as heavy metals, as suggested in many studies (Dominguez-Benetton et al., 2018; Yu, 2020; Huang et al., 2021b; Huang and Li Puma, 2022).

Within this overarching context, the present investigation was aimed at understanding the role of the EPS secreted by *Serratia marcescens* Q1 and *Stenotrophomonas* sp. YS1 with bidirectional EET via +0.5 V vs. standard hydrogen electrode, SHE (outward) or −0.5 V vs. SHE (inward) in the presence or in the absence of Cr(VI). These two EAB were selected since they are capable of simultaneous Cr(VI) removal and HCO_3^- metabolism when immobilized on the cathodes of dual-chamber BESs through inward EET (Xue et al., 2017; Qian et al., 2019; Sun et al., 2021; Huang et al., 2018; 2021a; 2021b). These two pure culture strains exhibit indigenous Cr(VI) endurance and opportunistic survival under low carbon sources or under nutrients barren conditions (Huang et al., 2021b). A direct comparison of the behavior of these two strains is beneficial to target the removal of heavy metals in either electron-donor or electron-acceptor deficient wastewaters. The dynamic change of circuital current and organic or inorganic carbon metabolism were correlated to electrochemical analysis (cyclic voltammetry (CV), differential pulse voltammetry (DPV)), and to the quantitative response of the EAB through the release of EPS (exoproteins and exopolysaccharides) with a compositional diversity, during both the outward or inward EET. The coulombic efficiency for inward and outward EET was also correlated to the EAB metabolic assimilation of Cr(VI) and HCO_3^- (inward) or acetate (outward). The findings of this study elucidate the role played by the EPS in response to Cr(VI) contamination, which plays an important role in the application of single-chamber BESs with different EET directions for the targeted removal of heavy metals in either electron-donor or electron-acceptor deficient wastewaters.

2 Materials and methods

2.1. Chemical reagents

All reagents were commercial products of analytical grade and obtained from Tianjin Bodi Chemistry Co., Ltd. Stock solutions of analytical reagents of acetate (50 mM), $NaHCO_3$ (100 mM) and $K_2Cr_2O_7$ (4 mM) were prepared with deionized water, respectively.

2.2. Microbial strains and culture medium

Gram-negative *S. marcescens* Q1 (GenBank MT982676.1) and *Stenotrophomonas* sp. YS1 (GenBank MZ703198) were isolated from the biocathodes of BESs operated over 2 − 3 years, originally inoculated with domestic wastewater and fed with a mix of carbon source HCO_3^- and heavy metals (e.g., Cr(VI)) to acclimatize the EAB to this feed (Huang et al., 2015a; Xue et al., 2017; Qian et al., 2019). Before inoculation, both Q1 and YS1 were cultured in Luria-Bertani medium overnight and at 30 ℃, and then washed in sterilized phosphate buffer solution for at least three times by centrifugation at 8000 × g for 5 min. These cell pellets were then added to a medium (previously autoclaved at 121 ℃ for 20 min) composed of NH_4Cl (5.8 mM), KCl (1.7 mM), $NaH_2PO_4{\cdot}H_2O$ (17.8 mM), Na_2HPO_4 (32.3 mM), a mineral solution (12.5 mL/L), a vitamin solution (12.5 mL/L) (Wang et al., 2012; Cheng et al., 2020), equivalent carbon molar numbers of acetate (outward, 5 mM) or $NaHCO_3$ (inward, 10 mM) as carbon sources (Molenaar et al., 2016; Jiang and Zeng 2019), and Cr(VI) (0.4 mM) to

produce a cell suspension (OD_{600}: 0.60). This solution was then employed as the electrolyte in the BESs. The concentration of Cr(VI) at 0.4 mM was selected on the basis of appropriate reduction by these EAB in the cathodes of dual-chamber BESs (Xue et al., 2017; Huang et al., 2021a; Sun et al., 2021). The initial pH and conductivity of the electrolyte solution of the BESs were fixed at 5.8 and 5.8 mS/cm, respectively (Huang et al., 2021a; Sun et al., 2021).

2.3. Electrode preparation and operation

All experiments were carried out using a three-electrode single-chamber BES constructed from Plexiglas (working volume: 40 mL; 2.9 cm inner diameter; 6.0 cm high). The porous graphite felt working electrode (1.0 cm × 1.0 cm × 0.5 cm; Sanye, Beijing, China) as anode (outward) or cathode (inward), was installed with a platinum wire counter electrode and an Ag/AgCl reference electrode, with both located 1.0 cm away from the working electrode (Zhao et al., 2009; Logan 2012). The selection of a working volume of 40 mL was mainly based on its frequent use in the range of 10 – 100 mL in literature (Xue et al., 2017; Huang et al., 2021a; 2022b; Yu et al., 2022). A glass tube (inner diameter: 0.8 cm; height: 24 cm; a total headspace: 12 mL) was installed at the top of the BES under the inward mode conditions to collect the gases evolved (e.g., H_2) as previously described (Wang et al., 2015). Electrolytes containing Q1 or YS1 (OD_{600}: 0.60) were sparged with a sterile-filtered CO_2 : N_2 (20 : 80) gas stream prior to transfer into the three-electrode system. The BES was operated with potentiostatic discharge or charge, at controlled electrode potentials of +0.5 V (outward)

157 or −0.5 V (inward) respectively using a potentiostat (VSP, BioLogic), with potentials
158 corrected to SHE, and the resulting currents measured. Based on the inherent redox
159 characters of acetate (outward), HCO_3^- (inward) and Cr(VI) in the electrolyte, the
160 potentials purposely set at +0.5 V vs. SHE (outward) or −0.5 V vs. SHE (inward), could
161 sufficiently guarantee the redox reactions, as shown by Zhao et al. (2009), Gary Grim
162 et al. (2020) and Huang et al. (2021). Before data collection, this system was gently
163 shaken in a table concentrator (ZHWY-304, Shanghai, China) at a rate of 30 rpm/min
164 to guarantee the bacterial deposition on the electrodes since the effluent contained
165 negligible bacteria at OD_{600} (Song et al., 2020; Huang et al., 2021a). All inoculation
166 and solution replacements were performed in an anaerobic glove box (YQX-II,
167 Xinmiao, Shanghai) equipped with a clean bench via an ultraviolet disinfection lamp.
168 Throughout the experiments, the purity of the electrolyte solution was periodically
169 examined using colony morphology via pure culture cultivation and cell morphology
170 via microscopy observation (Geelhoed and Stams, 2011). The reactors were protected
171 with aluminum foil to exclude light to avoid the growth of algae, and all reactors were
172 anaerobically operated in fed-batch mode and at a temperature of 23 ± 3 ℃.

173 Three control experiments were conducted: the first one was operated in the
174 absence of Cr(VI), which clarified the impact of Cr(VI) on the circuital current, the
175 amount and compositional diversity of EPS released by YS1 or Q1, and the utilization
176 of acetate (outward) or HCO_3^- (inward); The second (abiotic controls) was operated in
177 the absence of YS1 or Q1 inoculum, and reflected the effect of the EAB on the circuital
178 current, the removal of Cr(VI), and the utilization of acetate (outward) or HCO_3^-

(inward); The third was under open circuital conditions (OCCs) and thus in the absence of current, which elucidated the impact of circuital current on the removal of Cr(VI), the amount and compositional diversity of EPS, and the utilization of acetate (outward) or HCO_3^- (inward) by the EAB.

2.4. Measurement and analyses

The concentration of acetate (outward) in electrolyte and the residual hydrogen (inward) in the headspace was measured by gas chromatography (GC7900, Tianmei, China) as previously described (Kong et al., 2021; 2022). Briefly, a SE-54 cross-linking chromatographic column and thermal conductivity detector were used for hydrogen determination using N_2 as the carrier gas. The temperatures of the column and the injector were both 120 ℃. A PEG-20M column and flame ionization detector were employed for the quantification of acetate, using nitrogen as the carrier gas. The temperatures of the column and the injector were both 200 ℃. The concentration of HCO_3^- (inward) was determined using the national standard method (DZ/T 0064.49-93). The biomass deposited on the electrode and plankton cells in the electrolyte were quantified as previously described (Qian et al., 2019; Song et al., 2020). The residual oxygen in the electrolyte was monitored using a dissolved oxygen analyzer (JPBJ-609L, Leici, Shanghai, China) (Huang et al., 2015b). Cr(VI) analysis was based on the standard methods (APHA 1998).

The redox behaviors of outward or inward EET were analyzed using CV (VSP, BioLogic) with a standard three-electrode arrangement (working electrode, Pt counter

electrode, and an Ag/AgCl reference electrode) in the range of −0.8 ~ 0.6 V (vs. SHE) and at a scan rate range of 1 – 10 mV/s. These scan rates within the suggested range of 1 – 100 mV/s, ensured sufficient time for the response of the whole cell biocatalysts (Zhao et al., 2009; Huang et al., 2015a; 2015b). DPV, which is more sensitive than CV and is normally used to assess the electrochemical activities of the components on the electrodes (Zhao et al., 2009; Xiao et al., 2017; Kong et al., 2022), was further used to assess the likely redox-active components at a scan rate of 1 mV/s, an amplitude of 50 mV, and a pulse period of 1 s (Yang et al., 2017; Yi et al., 2021). The projected surface area (2.0 cm × 2.0 cm, 4.0 cm^2) of the Pt counter electrode, apparently larger than the area of the graphite felt working electrode (1.0 cm^2), exhibited less polarization loss and thus adapted well for the analysis of the working electrode (Wang et al., 2015).

The quantitative amount and compositional diversity of EPS released by either Q1 or YS1 on the electrodes or in the electrolyte, either with inward or with outward EET were evaluated at operational times of either 48 h or 120 h, and in the controls in the absence of either circuital current or Cr(VI). EPS was extracted following previous methods (Qian et al., 2019; Song et al., 2020; Huang et al., 2021a; Sun et al., 2021). The exoproteins and the exopolysaccharides in the EPS were measured by the Bradford assay and with the phenol-sulfuric acid method, respectively. Three-dimensional fluorescence excitation-emission matrix (FEEM) spectroscopy (F-7000, Hitachi, Japan) fitted with 1.0 cm quartz cell and a thermostat bath was used to characterize the EPS composition (Chen et al., 2003; Qian et al., 2019). The FEEM procedure and the definition of the EPS components (I, II, III, IV and V) are provided in Supplementary

223 Material (SM).

224

225 *2.5. Calculations*

226 During outward EET, the acetate fuel ($\alpha_{outward,total}$) was distributed among the
227 circuital current ($\int_0^t Idt$), Cr(VI) removal/reduction (α_{Cr}), biofilms or plankton cells
228 growth (α_{growth}), exoproteins release ($\alpha_{exoproteins}$) and exopolysaccharides release
229 ($\alpha_{exopolysaccharides}$) by the biofilms or plankton cells (Eqs. 1 − 5) (Wang et al., 2012).

230 Under inward EET conditions and using HCO_3^- as carbon source, the total
231 electrons ($\int_0^t Idt$) were mainly distributed for reduction of HCO_3^- to acetate ($\alpha_{acetate}$),
232 Cr(VI) removal/reduction (α_{Cr}), H_2 evolution (α_{H2}), residual oxygen reduction (α_{O2}),
233 biofilms or plankton cells growth (α_{growth}), exoproteins release ($\alpha_{exoproteins}$) and
234 exopolysaccharides release ($\alpha_{exopolysaccharides}$) by the biofilms or plankton cells (Eqs. 2 –
235 8) (Wang et al., 2012; Huang et al., 2015a; 2015b).

236 $$\alpha_{\text{outward,total}} = \frac{\alpha_1 \times (C_{0,\text{COD}} - C_{\text{t,COD}}) \times V \times \text{F}}{\text{M}_{\text{O2}}} \quad (1)$$

237 $$\alpha_{\text{growth}} = \frac{\alpha_1 \times \alpha_5 \times W_{\text{biomass}} \times \text{F}}{\text{M}_{\text{O2}}} \quad (2)$$

238 $$\alpha_{\text{exoproteins}} = \frac{\alpha_1 \times \alpha_7 \times W_{\text{exoproteins}} \times \text{F}}{\text{M}_{\text{O2}}} \quad (3)$$

239 $$\alpha_{\text{exp olysacchrides}} = \frac{\alpha_1 \times \alpha_6 \times W_{\text{expolysacchrides}} \times \text{F}}{\text{M}_{\text{O2}}} \quad (4)$$

240 $$\alpha_{\text{cr(VI)}} = \alpha_4 \times \Delta C_{\text{Cr(VI)}} \times V \times \text{F} \quad (5)$$

241 $$\alpha_{\text{acetate}} = \alpha_2 \times C_{\text{t,acetate}} \times V \times \text{F} \quad (6)$$

242 $$\alpha_{\text{H}_2} = \alpha_3 \times h \times \text{F} \quad (7)$$

243 $$\alpha_{\text{O}_2} = \alpha_1 \times C_{t,oxygen} \times \text{F} \quad (8)$$

244 Where I is the circuit current (A); F is the Faraday's constant (96485 C/mol

245 electron); M_{O2} is the relative molecule weight of O_2 (32 g/mol); V is the electrolyte
246 volume (L); t is the operation time (s); α_1 (4 mol/mol), α_2 (8 mol/mol), α_3 (2 mol/mol),
247 and α_4 (3 mol/mol) are the number of electrons required for O_2 reduction (outward or
248 inward), CH_3COO^- production (inward), hydrogen evolution and Cr(VI) reduction,
249 respectively; $\Delta C_{Cr(VI)}$ is the difference between the initial and the final Cr(VI)
250 concentrations in the electrolyte (mol/L); α_5, α_6 and α_7 are the transfer parameters of
251 1.42 mg COD/mg dry weight (DW), 1.07 g COD/g glucose and 1.47 g COD/g
252 bovine serum albumin, respectively (Erable et al., 2018); h is the net moles of hydrogen
253 in the headspace; $W_{biomass}$ (g), $W_{exopolysaccharides}$ (g) and $W_{exoproteins}$ (g) are the amounts of
254 biomass, exopolysaccharides and exoproteins, respectively.

255 The values reported were averaged based on the statistics analysis of three
256 replicate experiments for each of the duplicate reactors. One-way ANOVA in SPSS 19.0
257 was used to analyze the statistical differences among the data at significance levels of
258 $p < 0.05$.

259

260 **3 Results and discussion**

261 *3.1 Performance during outward or inward EET*

262 The results (Fig. 1A) shows strain YS1 as more efficient than Q1 as outward
263 electron donor in the presence of Cr(VI). After a 29 h lag start-up time, a steep increase
264 in current was observed that reached a maximum of 8.0 μA (20 mA/m^2) at 48 h.
265 Conversely, the current with Q1 reached a plateau at 4.7 – 5.2 μA (11 − 13 mA/m^2) at
266 24 – 58 h with a short lag start-up time (12 h) (Fig. 1A). The faster rate of acetate

utilization observed under CCCs than OCCs (Fig. 1C) reflected the positive impact of circuital current on both strains with outward EET, whereas the similar Cr(VI) removals under CCCs and OCCs (Fig. 1D) suggested the dominant role of Cr(VI) bio-adsorption over the reduction kinetics. The controls in the absence of Cr(VI), shortened the lag start-up time (YS1: 24 h; Q1: 5 h), increased the circuital current (YS1: 8.5 – 8.7 μA; Q1: 5.8 – 6.5 μA) (Fig. 1B) and the rate of acetate utilization (Fig. 1E), reflecting the unfavorable role of Cr(VI) in the EAB biofilms outward EET. These differences in start-up times and peak currents suggest that multiple outward electron transport pathways are associated with the YS1 and Q1, and that a regulatory mechanism of these strains was taking place. Other EAB such as *Geobacter sulfurreducens* and *Geoalkalibacter ferrihydriticus* in the absence of Cr(VI) also reportedly exhibited similar results (Yoho et al., 2014; 2015). The much lower currents (0.20 – 0.24 μA) in the abiotic controls (Fig. 1A and B), reflected the tremendous importance of these biotic catalysts in the outward EET. Q1 was more responsive that YS1 on outward EET in the absence of Cr(VI) (Fig. 1A and B), since the percentage increase in circuital currents was higher (26.0% vs. 8.8%) and the lag start-up times were lower (Q1: 5 h vs. 12 h; YS1: 24 h vs. 29 h). The circuital currents were higher than or comparable to those observed in the absence of Cr(VI) (*Shewanella woodyi*: 0.2 μA; *Ardenticatena maritima* and *Comamonas testosterone*: 8 – 11 μA) (Tian et al., 2017; Kawaichi et al., 2018; Yu et al., 2015), but somewhat lower than those observed with *Shewanella oneidensis* (18 − 22 μA) in the presence of Cr(VI) (Xafenias et al., 2011; Cheng et al., 2019).

Under inward EET conditions, significant higher currents than under outward EET

were observed with Q1 (165 μA), which was also higher than YS1 (118 μA) (Fig. 1F). These results demonstrated the switchable nature of these two strains, but this time the absorption of electrons was more efficient with Q1 rather than with YS1. These currents were higher than the model *Shewanella oneidensis* of 100 μA during inward EET in the presence of Cr(VI) (Cheng et al., 2019). This along with its lower currents than *Shewanella oneidensis* during outward EET demonstrated the larger differentiation of both strains between outward and inward EET than the *Shewanella oneidensis*. These different circuital currents, complemented by HCO_3^- utilization (Fig. 1H) and Cr(VI) removal (Fig. 1I), suggested a more efficient behavior of Q1 than YS1 for directing a higher amount of electrons for both HCO_3^- and Cr(VI), as also revealed from the charge distribution analysis. The invariably increased circuital current in the presence of Cr(VI) (Fig. 1F vs. Fig. 1G and J) is supported by the higher amount of electron acceptors in the electrolyte, as summarily reviewed by He et al. (2015).

The results of both forward and inward EET indicate that both strains YS1 and Q1 exhibit bidirectional and switchable electron transfer, although electron uptake was more significant than electron donation. In the presence of Cr(VI), the biofilm YS1 outward EET was higher than Q1, while conversely Q1 inward EET was higher than YS1. Similar bidirectional EET behavior has been observed in other bacterial strains including *Shewanella oneidensis*, *Shewanella woodyi*, *Desulfovibrio caledoniensis* and *Alcaligenes faecalis* in the absence of Cr(VI) (Tian et al., 2017; Yu et al., 2018; Zang et al., 2022; Jia et al., 2023).

311 *3.2 CVs at different scan rates*

312 The dynamic electrochemical characterization of both outward (Fig. 2A − D) and
313 inward (Fig. 2E − H) EET of JY1 (Fig. 2A, B, E and F) and Q1 (Fig. 2C, D, G and H)
314 biofilms in the presence (Fig. 2A, C, E and G) or in the absence (Fig. 2B, D, F and H)
315 of Cr(VI) at sweep speeds of 1 – 10 mV/s, invariably suggested a good proportional
316 relationship between the peak current and the sweep speed (R^2: presence of Cr(VI): JY1:
317 0.9923, Q1: 0.9973; absence of Cr(VI): JY1: 0.9987, Q1: 0.9998) (Fig. 3A and B),
318 instead of the peak current and square root of scan rate (R^2: presence of Cr(VI): JY1:
319 0.9626, Q1: 0.9851; absence of Cr(VI): JY1: 0.9849, Q1: 0.9776) (Fig. S1). In
320 consequence, the redox reactions during the outward and inward EET resulted from an
321 electron-exchange process mediated by the adsorbed species and controlled by typical
322 surface adsorbed processes, regardless of the presence of Cr(VI), while diffusion and
323 migration were not major contributors to the redox reactions at the interface. Such result
324 is consistent with the behavior of other EAB individual outward or inward EET with or
325 without Cr(VI) (Huang et al., 2015a; 2015b; Tian et al., 2017; Yu et al., 2018; Wu et al.,
326 2022). The decreased CV gradient in the scans of the biotic electrode with outward EET
327 compared to the absence of Cr(VI) (acetate oxidation, YS1: 0.0269 vs. 0.0290, Fig. 3A;
328 Q1: 0.0220 vs. 0.0239, Fig. 3B), along with those inward EET (HCO_3^- reduction, YS1:
329 0.0247 vs. 0.0262, Fig. 3C; Q1: 0.0189 vs. 0.0216, Fig. 3D), invariably confirmed the
330 altered kinetic behaviors of both YS1 and Q1 outward and inward biofilms due to the
331 presence of Cr(VI), consistent with the results shown in Fig. 1. The invariable steeper
332 gradients of the JY1 than the Q1 outward (0.0269 vs. 0.0220) (Fig. 3A and B) or inward

(0.0247 vs. 0.0189) (Fig. 3C and D) biofilms EET suggested the more adaptive and robust behavior of JY1 over Q1 biofilms bidirectional EET under the presence of Cr(VI) heavy metal.

3.3 Comparison of biotic and abiotic CV and DPV

It is generally agreed that the more negative reductive onset potentials (inward) or the more positive oxidative onset potentials (outward) imply the increase in the thermodynamic overall free energy of the corresponding electron transfer reactions, whereas lower reductive peak currents (inward) or lower oxidative peak currents (outward) suggest varying degrees of dynamic mass transfer inhibition of the corresponding electron transfer reactions (Zhao et al., 2009; He et al., 2015; Dominguez-Benetton et al., 2018; Huang et al., 2021b). In agreement with the results in Fig. 1C and E, invariably, the presence of Cr(VI) shifted the acetate oxidation onset potentials of YS1 or Q1 to more positive values from 0.245 V to 0.255 V (Fig. 4A; Table S1), while as expected the abiotic controls did not show any acetate oxidation peak. This observation along with the diminished oxidation peak currents (YS1: 0.028 mA vs. 0.032 mA; Q1: 0.023 mA vs. 0.026 mA) (Fig. 4A and B; Table S1), in concert confirmed an increase of the thermodynamic overall free energy and dynamically an increment mass transfer inhibition of the catalytic YS1 and Q1 outward EET in response to the presence of Cr(VI), consistent with the results in Fig. 1A and B, Fig. 2A – D, and Fig. 3A and B. An indication that intrinsic different EPS components, such as free riboflavin or riboflavin bounded with extracellular cytochrome *c,* were involved into

355 indirect outward EET, is given by the invariability of the oxidation peak potentials in
356 the DPV plots regardless of the presence of Cr(VI) (YS1: 0.039 V; Q1: −0.067 V) (Fig.
357 4E and F; Table S1), and corresponding decreased oxidation peak currents (YS1: 0.602
358 mA vs. 0.624 mA, Q1: 0.523 mA vs. 0.547 mA; Fig. 4E and F; Table S1), as
359 subsequently discussed, similar to the observation with other EAB with outward EET
360 (Xiao et al., 2017; Min et al., 2017; Yi et al., 2021).

361 With regard to inward EET, Q1 rather than YS1 more efficiently catalyzed the
362 reduction of HCO_3^- in the presence of Cr(VI), evidenced by a less negative inorganic
363 carbon reduction onset potential (−0.445 V vs. −0.465 V) (Fig. 4C; Table S1), consistent
364 with the results in Fig. 1H, implying a more significant reduction of the overall free
365 energy of the electron transfer reactions in Q1 compared to YS1, due to bacterial
366 interactions with the electrode surface (Huang and Li Puma, 2022). In the controls in
367 the absence of Cr(VI), however, the less negative inorganic carbon reduction onset
368 potentials with higher reduction peak currents (YS1: −0.456 V vs. −0.465 V, 0.046 mA
369 vs. 0.044 mA; Q1: −0.436 V vs. −0.445 V, 0.079 mA vs. 0.062 mA) (Fig. 4C and D;
370 Table S1) reflected the invariable negative impact of Cr(VI) on both strains inward EET
371 for inorganic carbon reduction, consistent with the results in Fig. 1H and J. The more
372 significant decrease of the inorganic carbon reduction peak currents observed with Q1
373 than YS1 (21.5% vs. 4.3%) due to the presence of Cr(VI) (Fig. 4C and D; Table S1),
374 suggested a more substantial increase of the dynamic mass transfer resistance for Q1
375 than YS1 biofilms during inward EET. The crucial role of the biotic cathode is
376 exemplified by absence of inorganic carbon reduction peak in the abiotic controls with

(Fig. 4C; Table S1) or without (Fig. 4D; Table S1) Cr(VI). The same Cr(VI) reduction onset potential at 0.204 V with higher reduction peak currents of Q1 than YS1 (0.036 mA vs. 0.025 mA) (Fig. 4C; Table S1), suggested a similar intrinsic thermodynamic behavior and a lower dynamic mass transfer resistance for Q1 than YS1 biofilms during inward EET for Cr(VI) reduction, consistent with the results in Fig. 1I. DPV results showed the appearance of two similar reduction peak potentials (YS1: 0.024 V and −0.187 V; Q1: 0.019 V and −0.186 V) regardless of the presence of Cr(VI) (Fig. 4G and H; Table S1), suggesting that the components of outer membrane *c*-type cytochromes and protein-bound flavins could remained unaltered, respectively for the YS1 and Q1 biofilms during inward EET, with or without Cr(VI). Outer membrane *c*-type cytochromes and/or protein-bound flavins have been proven to drive inward EET in many other EAB (e.g., *Shewanella oneidensis*, *Bacillus* sp., *Pichia stipites*, *Shewanella loihica* and *Listeria monocytogenes*) using multiple techniques including electrochemistry, spectroscopy, atomic force microscopy, and/or molecule microbiology (Xiao et al., 2017; Cheng et al., 2020; Yi et al., 2021; Huang and Li Puma, 2022). The invariably larger reduction peaks (Fig. 4G and H) over the oxidation peaks (Fig. 4E and F) with both YS1 or Q1 implies the involvement of more diverse inward EET pathways, similarly to the behavior of other EAB such as *Shewanella loihica* (Yi et al., 2021).

Collectively, these results demonstrated that inward EET was more significant in Q1, while outward EET was more significant in YS1.

3.4 EPS secretion

The presence of a circuital current invariably stimulated both YS1 and Q1 biofilms strains to produce exoproteins despite this was more significant with inward EET (Fig. 5A and B). Thus, the higher currents observed under inward EET (Fig. 4) is consistent with the higher amount of redox-active substances harbored within the exoproteins material (Xiao et al., 2017; Yu 2020; Huang and Li Puma, 2022). However, in the presence of Cr(VI) the release of exoproteins at 48 h (Fig. 5A and B) decreased, reflecting a contrasting effect of Cr(VI) also shown on the current.

With regard to the production of exopolysaccharides which facilitate cell aggregation and adhesion as well as the maintenance of cell envelop integrity, both circuital current and Cr(VI) improved the amount produced by both YS1 and Q1 biofilms during outward EET (Fig. 5C). However, during inward EET, only Cr(VI) induced the release of exopolysaccharides, while the circuital current had negligible effect (Fig. 5D). Thus, the two biofilm strains exerted variable regulative manipulation strategies releasing different amounts of exoproteins and exopolysaccharides when responding to an external circuital current and/or Cr(VI) during their switchable EET, as reported by Huang and Li Puma (2022). Moreover, such a regulatory mechanism is more significantly exerted on the biofilms rather than in the plankton cells, given that the amount of exoproteins and exopolysaccharides in the latter was significantly smaller (Fig. S2). It should be observed that, the ratios of exoproteins and exopolysaccharides was severely suppressed by the presence of Cr(VI), while it was increased by circuital current during inward EET (Fig. 5F). In contrast, the ratios of exoproteins and

exopolysaccharides was approximately unaltered under outward EET (Fig. 5E), as hypothesized by Huang and Li Puma (2022).

3.5 YS1 and Q1 biofilms EPS composition

FEEM spectroscopy displayed the EPS components secreted by YS1 and Q1 biofilms during outward or inward EET in the presence of Cr(VI) at operational times of 48 h (Figs. 6 and 7) or 120 h (Fig. S3; Fig. 7). These results varied significantly among the YS1 and Q1, and depended on the direction of EET, the circuital current, the presence of Cr(VI), and the operational time.

The presence of Cr(VI) and circuital current significantly stimulated YS1 biofilms outward EET to release the highest amount of fulvic acid-like materials (Region III) rather than the other four components (Regions I and II: simple aromatic proteins such as tyrosine; Region IV: soluble microbial byproduct-like material; Region V: humic acid-like materials) at 48 h (p: 0.0001 – 0.0011) or 120 h (p: 0.0036 – 0.021) (Fig. 6A and 7A; Fig. S3A). Fulvic acid-like and humic acid-like substances are both humic substances, which have been proven to facilitate EET in many BESs as electron mediators (Huang Huang and Angelidaki 2008). As consequence, components III with involved outward EET cannot be excluded. However, in the absence of Cr(VI) the highest components were IV (p: 0.002 – 0.011) (Fig. 6C, 6D and 7E; Fig. S3B), which might be somewhat related with the free riboflavin or riboflavin bounded with outer membrane *c*-type cytochromes (Fig. 4E; Table S1), similar to the observation in other BESs (Zhao et al., 2022). Similarly, low II and III materials (p: 0.47) observed under

443 OCCs (Fig. 6B, 6D and 7E) might imply their consistence in the absence of circuital
444 current. With regard to Q1, similar higher quantities of Regions II and III components
445 were measured in the presence of Cr(VI) and circuital current at 48 h (p: 0.20) or 120 h
446 (p: 0.20) (Fig. 6E and 7B; Fig. S3C), while in the absence of Cr(VI) appreciable higher
447 V, III and II components were observed (p: 0.003 – 0.023) (Fig. 6G, 6H and 7F; Fig.
448 S3D), and under OCCs the highest components were II (p: 0.008 – 0.049) (Fig. 6F, 6H
449 and 7F). Thus, it can be concluded that the compositional amount and diversity of
450 the EPS composites is strongly dependent on the EAB strain, in the presence or in the
451 absence of circuital current and Cr(VI) during the process of outward EET.

452 Under inward EET, YS1 biofilms released the highest components III than the
453 other materials and those under OCCs (p: 0.0001 – 0.011) (Fig. 6I and 7C; Fig. S3E),
454 whilst the highest component was II in the absence of Cr(VI) (p: 0.0012 – 0.032) (Fig.
455 6J, 6K, 6L and 7G; Fig. S3F). For Q1, however, the higher III (p: 0.0002 – 0.0033) and
456 V (p: 0.0001 – 0.0021) components in the presence of Cr(VI) and circuital current (Fig.
457 6M and 7D; Fig. S3G), might explain the higher amounts of exoproteins (Fig. 5B) and
458 exopolysaccharides (Fig. 5D) observed. This along with the significant higher V
459 component in the absence of Cr(VI) (p: 0.014 – 0.045) (Fig. 6O and 7H; Fig. S3H)
460 compared to OCCs with (Fig. 6N and 7D) or without (Fig. 6P and 7H) Cr(VI) may
461 suggest that V does not contribute to the secretion of high amount of
462 exopolysaccharides (Fig. 5D).

463 It is noteworthy that the general higher amount of components III over the other
464 materials regardless of the EET direction for both bacterial strains (Fig. 7A – D), might

imply the harboring of shiftable substances not limited to the free riboflavin or riboflavin bounded with outer membrane *c*-type cytochromes. Collectively, these results shows that bidirectional EET in these bacterial strains is upregulated by the secretion of varying amount of EPS (exoproteins and exopolysaccharides) with compositional diversity, which depends on the electron transfer direction (inward or outwards) and on the presence of circuital current and a heavy metal such as Cr(VI) in this study, opening up interesting opportunities for manipulating, exploiting and tuning the EAB response in BESs.

3.6 Charge distribution

The presence of Cr(VI) induced both biofilms strains outward EET to extract less electrons from acetate oxidation at either 48 h (YS1: 0.30 ± 0.00 C vs. 0.49 ± 0.01 C; Q1: 0.54 ± 0.01 C vs. 0.71 ± 0.01 C) or 120 h (YS1: 1.29 ± 0.02 C vs. 1.53 ± 0.01 C; Q1: 1.19 ± 0.02 C vs. 1.46 ± 0.01 C) (Fig. 8A and B), consistent with the result in Fig. 1A, B, F and G. Accordingly, more electrons equivalent were directed to produce exoproteins and exopolysaccharides at 120 h than at 48 h (Fig. 8A and B), while the concentration of Cr(VI) progressively decreased in the electrolyte (Fig. 1D) consistent with the physiological release of EPS by both biofilms strains during outward EET (Fig. 5A and C).

Appreciably more electrons were directed via inward (Fig. 8C and D) than outward (Fig. 8A and B) EET, as previously observed in the results shown in Fig. 1A, B, F and G. Therefore, the Q1 biofilm absorbed a higher amount of electrons than YS1 from the

electrode via inward EET, which were utilized for HCO_3^- reduction to acetate (48 h: 2.30 ± 0.11 C vs. 1.04 ± 0.04 C; 120 h: 2.66 ± 0.04 C vs. 1.36 ± 0.16 C) with similar low residual amount of H_2 (as an indirect mediator) (48 h: 0.18 ± 0.03 − 0.23 ± 0.02 C; 120 h: 0.85 ± 0.08 – 1.38 ± 0.11 C) in the presence of Cr(VI) (Fig. 8C). The higher production of acetate than the controls in the absence of Cr(VI) (Fig. 8C and D), illustrated the superior biocatalytic properties of Q1 over YS1 for the transformation of HCO_3^- to acetate, consistent with the results in Fig. 1H and supported by its efficient Cr(VI) removal with simultaneous production of acetate from HCO_3^- in the cathodes of dual-chamber BESs (Huang et al., 2021a). The presence of Cr(VI) directed a higher fraction of electrons towards the bacterial release of exopolysaccharides and a smaller fraction towards the secretion of exoproteins at 48 h (Fig. 8C and D), consistent with the results in Fig. 5B and D. Both strains preferentially consumed a higher amount of electrons for Cr(VI) reduction (1.61 ± 0.01 – 1.68 ± 0.01 C) and biofilms growth (1.09 ± 0.60 – 1.26 ± 0.44 C) at a prolonged operational time of 120 h (Fig. 8C). The electron charges for release of exoproteins in the Q1 biofilms were the same at 48 h and at 120 h, and were higher than those observed with YS1 (Fig. 8C), consistent with the results in Fig. 5B. These results jointly demonstrated the EAB biofilms-based variable pathways of electron uptake and distribution along with modulation of EPS release as a function of operational time.

With regards to planktons and regardless of outward or inward EET with or without Cr(VI), all fractions of YS1 and Q1 biomass, exopolysaccharides and exoproteins were always lower than those of YS1 and Q1 biofilms (Fig. 8), consistent

with the generally agreed dominant contribution of biofilms instead of planktons to outward or inward EET in BESs (He et al., 2015; Dominguez-Benetton et al., 2018; Jiang et al., 2019; Huang and Li Puma 2022a). With outward EET, the growth of planktonic cells of Q1 and YS1was favored by Cr(VI) at 48 h rather than at 120 h (Fig. 8A), and contrasted sharply with the results in the absence of Cr(VI) (Fig. 8B), implying the influential role of Cr(VI) with operational time. However, the growth of planktonic cells of Q1 was significantly inhibited in comparison to YS1 during inward EET and in the presence of Cr(VI) (Fig. 8C and D). These results along with compositional diversity of EPS in the planktonic YS1 and Q1 during outward or inward EET with or without Cr(VI) at 48 h (Fig. S4 and S6) or 120 h (Fig. S5 and S6), demonstrated the presence of diverse pathways of electron uptake and distribution by EAB planktons.

It has yet to be demonstrated that the outward or inward EET of YS1 and Q1 biofilms and planktons is exactly correlated with cell respiration regardless of the presence of Cr(VI), and still a variety of other mechanisms can be proposed on the catalytic inward or outward behavior of the bidirectional YS1 or Q1 strains (Wang et al., 2012; Xue et al., 2017; Qian et al., 2019; Huang et al., 2021a; 2021b; Gai et al., 2024).

The results herein shown give new insights and an in-depth quantitative appreciation of the fate of the electrons in these Cr(VI)-tolerant EAB, and provide a comprehensive appreciation of the tuning of EPS release in response to Cr(VI) stressing conditions and circuital current, thus advancing our knowledge on these metallurgical EAB with bidirectional EET behavior. This is of tremendous importance as the

development of both bioanodes and biocathodes have gained increasing attention as novel routes for assimilating reductive organics or for the removal of a range of oxidative heavy metals in newly developed single-chamber BESs (Dominguez-Benetton et al., 2018; Jiang and Zeng 2019; Huang and Li Puma 2022a; Huang et al., 2023; Gai et al., 2024).

Q1 favored inward EET while YS1 preferred outward EET in the presence of Cr(VI), despite both strains were capable of bidirectional EET. The diverse EET behaviors of YS1 and Q1 along with their opportunistic metabolism of organics (acetate) or inorganic (HCO_3^-) carbon sources, enriches the family of EAB capable of bidirectional EET. This study provided a plausible approach of exploiting YS1 or Q1-fed single-chamber BESs for treatment of Cr(VI) contaminated wastewaters. The variable quantities and composition of the EPS released by Q1 and YS1 during inward or outward EET in response to the external presence of Cr(VI) and circuital current provided an opportunity for regulative manipulation of these bidirectional EAB via adaptive electrochemically-tunable EPS components.

This study and others (Jiang et al., 2019; Huang et al., 2021b; Huang and Li Puma 2022a), demostrate that bidirectional EAB may show identical or different pathways during outward or inward EET. While *Shewanella oneidensis* has identical outward and inward EET pathways with the employment of outer membrane electron conduit MtrCAB for electron transfer, *Geobacter sulfurreducens* exhibited completely different inward and outward EET mechanisms based on the involvement of diverse electron transmitters around the inner membrane, the periplasm and the outer membrane

553 (Kouzuma et al., 2010; Jiang and Zeng 2019; Wu et al., 2022). Considering the general
554 complex energy-coupling factor transporter with functionally diverse redox activities
555 in many bacterial cell envelopes and extracellular surroundings, further investigations
556 on bidirectional small-molecule transport across the cytoplasmic membrane and the
557 assembly of redox-active proteins within the cell envelope and surrounding EPS along
558 with expression of associated functional genes in these metallurgical EAB, are still
559 needed.

560 It is still difficult to accurately discriminate and interpretate the true compositional
561 and structural properties of the EPS molecules based on current chemical analysis or
562 EEM techniques. The diverse composition of the EPS physiologically released by YS1
563 and Q1 during inward or outward EET in response to the external presence of Cr(VI)
564 and circuital current, appeals new molecular level measurement techniques along with
565 the in situ spectroscopic high-resolution characterization techniques, which should
566 make it possible to better map these interactions. Moreover, cytochrome profiling of
567 YS1 and Q1 could provide further insights on the differential expression of redox
568 enzymes in the presence of Cr(VI) with or without circuital current.

569

570 **4 Conclusions**

571 This study has proven that *Stenotrophomonas* sp. YS1 and *S. marcescens* Q1 EAB
572 are capable of bidirectional EET in the presence of a circuital current and Cr(VI).
573 Inward EET was more significant in Q1 while outward EET was more significant in
574 YS1. Accordingly, the amount and compositional diversity of the EPS released by Q1

and YS1 biofilms and planktons during inward or outward EET varied in response to the external presence of Cr(VI) and circuital current, suggesting the regulative manipulation of these EAB with bidirectional EET via adaptive electrochemically-tunable EPS components. During inward EET the two strains produced a higher amount of EPS as a defense mechanism over Cr(VI) stress, facilitating electron transfer through the production of exoproteins and cell adhesion and integrity through the production of exopolysaccharides. The fully exact correlation of EPS components to the operating conditions remains difficult to be deciphered and needs further investigations. These results show that bidirectional EET in bacterial strains is upregulated by the secretion of varying amount of EPS (exoproteins and exopolysaccharides) with varying composition which depends on the EET direction (inward or outwards) and on the presence of circuital current and heavy metal such as Cr(VI), opening up interesting opportunities for manipulating, exploiting and tuning the EAB response in BESs. The findings of this study elucidate the role played by the EPS in response to Cr(VI) contamination, which plays an important role in the application of single-chamber EAB with different EET directions for the targeted removal of heavy metals in either electron-donor or electron-acceptor deficient wastewaters.

Declaration of competing interest

There are no conflicts to declare.

Data availability

Data will be made available on request.

Acknowledgements

The authors gratefully acknowledge financial support from the National Natural Science Foundation of China (Nos. 22276025 and 52070032), and the Key Laboratory of Industrial Ecology and Environmental Engineering (KLIEEE-22-04).

References

American Public Health Association, American Water Works Association, Water Pollution Control Federation, Standard methods for the examination of water and wastewater, 20th ed., American Public Health Association, Washington, DC, 1998.

Cai Z, Huang L, Quan X, Zhao Z, Shi Y, Li Puma G. Acetate production from inorganic carbon (HCO_3^-) in photo-assisted biocathode microbial electrosynthesis systems using WO_3/MoO_3/g-C_3N_4 heterojunctions and *Serratia marcescens* species. Appl Catal B-Environ 267 (2020) 118611. https://doi.org/10.1016/j.apcatb.2020.118611

Chen W, Westerhoff P, Leenheer JA, Booksh K. Fluorescence excitationemission matrix regional integration to quantify spectra for dissolved organic matter. Environ Sci Technol 37 (2003) 5701-5710. https://doi.org/10.1021/es034354c

Cheng ZH, Xiong JR, Min D, Cheng L, Liu DF, Li WW, Jin F, Yang M, Yu HQ. Promoting bidirectional extracellular electron transfer of *Shewanella oneidensis* MR-1 for hexavalent chromium reduction via elevating intracellular cAMP level. Biotechnol Bioeng 117 (2020) 1294-1303. https://doi.org/10.1002/bit.27305

Dominguez-Benetton X, Chandrakant Varia J, Pozo G, Modin O, ter Heijne A, Fransaer J, Rabaey K. Metal recovery by microbial electro-metallurgy. Prog Mater Sci 94 (2018) 435-461. https://doi.org/10.1016/j.pmatsci.2018.01.007

Erable B, Oliot M, Lacroix R, Bergel A, Serov A, Kodali M, Santoro C, Atanassov P. Iron-nicarbazin derived platinum group metal-free electrocatalyst in scalable-size air-breathing cathodes for microbial fuel cells. Electrochim Acta 277 (2018) 127-135. https://doi.org/10.1016/j.electacta.2018.04.190

Gai Z, Zhang Y, Wang Q, Shi Y, Yang J, Tan F, Huang L. Combined effect of temperature and illumination on treatment of etching terminal wastewater in single-chamber microbial electrolysis cells. Chem Eng Sci 298 (2024) 120399. https://doi.org/10.1016/j.ces.2024.120399

Gary Grim R, Huang Z, Guarnieri MT, Ferrell III JR, Tao L, Schaidle JA. Transforming the carbon economy: challenges and opportunities in the convergence of low-cost electricity and reductive CO_2 utilization. Energy Environ Sci 13 (2020) 472-494. https://doi.org/10.1039/c9ee02410g

Geelhoed JS and Stams AJM. Electricity-assisted biological hydrogen production from acetate by *Geobacter sulfurreducens*. Environ Sci Technol 45 (2011) 815-820. https://doi.org/10.1021/es102842p

He C, Mu Z, Yang H, Wang Y, Mu Y, Yu H. Electron acceptors for energy generation in microbial fuel cells fed with wastewaters: a mini-review. Chemosphere 140 (2015) 12-17. https://doi.org/10.1016/j. chemosphere.2015.03.059

Huang L and Angelidaki I. Effect of humic acids on electricity production integrated with xylose degradation in a microbial fuel cell. Biotechnol Bioeng 100 (2008) 413-422. https://doi.org/10.1002/bit.21786

Huang L, Wang Q, Jiang L, Zhou P, Quan X, Logan BE. Adaptively evolving bacterial communities for complete and selective reduction of Cr(VI), Cu(II), and Cd(II) in biocathode bioelectrochemical systems. Environ Sci Technol 49 (2015a) 9914-9924. https://doi.org/10.1021/acs.est.5b00191

Huang L, Liu Y, Yu L, Quan X, Chen G. A new clean approach for production of cobalt dihydroxide from aqueous Co(II) using oxygen-reducing biocathode microbial fuel cells. J Clean Prod 86 (2015b) 441-446. https://doi.org/10.1016/j.jclepro.2014.08.018

Huang L, Zhou P, Quan X, Logan BE. Removal of binary Cr(VI) and Cd(II) from the catholyte of MFCs and determining their fate in EAB using fluorescence probes. Bioelectrochemistry 122 (2018) 61-68. https://doi.org/10.1016/j.bioelechem.2018.02.010

Huang L, Song S, Cai Z, Zhou P, Li Puma G. Efficient conversion of bicarbonate (HCO_3^-) to acetate and simultaneous heavy metal Cr(VI) removal in photo-assisted microbial electrosynthesis systems combining WO_3/MoO_3/g-C_3N_4 heterojunctions and *Serratia marcescens* electrotroph. Chem Eng J 406 (2021a) 126786. https://doi.org/10.1016/j.cej.2020.126786

Huang L, Xing X, Zhou P, Li Puma G. Mixotrophic bacteria for environmental detoxification of contaminated waste and wastewater. Appl Microbiol Biotechnol 105 (2021b) 6627-6648. https://doi.org/10.1007/s00253-021-11514-5

Huang L, Kong W, Song S, Quan X, Li Puma G. Treatment of industrial etching terminal wastewater using $ZnFe_2O_4$/g-C_3N_4 heterojunctions photo-assisted cathodes in single-chamber microbial electrolysis cells. Appl Catal B-Environ 335 (2023) 122849. https://doi.org/10.1016/j.apcatb.2023.122849

Huang L and Li Puma G. Physiological response of electroactive bacteria via secretion of extracellular polymeric substances in microbial electrochemical processes: a review. Curr Opin Electrochem 36 (2022a) 101168. https://doi.org/10.1016/j.coelec.2022.101168

Huang L, Wan H, Song S, Liu D, Li Puma G. Complete removal of heavy metals with simultaneous efficient treatment of etching terminal wastewater using scaled-up microbial electrolysis cells. Chem Eng J 439 (2022b) 135763. https://doi.org/10.1016/j.cej.2022.135763

Jiang Y and Zeng RJ. Bidirectional extracellular electron transfers of electrode-biofilm: Mechanism and application. Bioresour Technol 271 (2019) 439-448. https://doi.org/10.1016/j.biortech.2018.09.133

Kong W, Huang L, Quan X, Zhao Z, Li Puma G. Efficient production of acetate from inorganic carbon (HCO_3^-) in microbial electrosynthesis systems incorporating Ag_3PO_4/g-C_3N_4 anaerobic photo-assisted biocathodes. Appl Catal B-Environ 284 (2021) 119696. https://doi.org/10.1016/j.apcatb.2020.119696

Kong W, Huang L, Quan X, Li Puma G. Synergistic induced charge transfer switch by oxygen vacancy and pyrrolic nitrogen in $MnFe_2O_4$/g-C_3N_4 heterojunctions for

efficient transformation of bicarbonate to acetate in photo-assisted MES. Appl Catal B-Environ 307 (2022) 121214. https://doi.org/10.1016/j.apcatb.2022.121214

Kouzuma A, Meng XY, Kimura N, Hashimoto K, Watanabe K. Disruption of the putative cell surface polysaccharide biosynthesis gene SO3177 in *Shewanella oneidensis* MR-1 enhances adhesion to electrodes and current generation in microbial fuel cells. Appl Environ Microbiol 76 (2010) 4151-4157. https://doi.org/10.1128/AEM.00117-10

Logan BE. Essential data and techniques for conducting microbial fuel cell and other types of bioelectrochemical system experiments. ChemSusChem 5 (2012) 988-994. https://doi.org/10.1002/cssc.201100604

Min D, Cheng L, Zhang F, Huang X, Li D, Liu D, Lau TC, Mu Y, Yu H. Enhancing extracellular electron transfer of *Shewanella oneidensis* MR-1 through coupling improved flavin synthesis and metal reducing conduit for pollutant degradation. Environ Sci Technol 51 (2017) 5082-5089. https://doi.org/10.1021/acs.est.6b04640

Nguyen VK, Park Y, Yu J, Lee T. Simultaneous arsenite oxidation and nitrate reduction at the electrodes of bioelectrochemical systems. Environ Sci Pollut Res 23 (2016) 19978-19988. https://doi.org/10.1007/s11356-016-7225-9

Qian Y, Huang L, Zhou P, Tian F, Li Puma G. Reduction of Cu(II) and simultaneous production of acetate from inorganic carbon by *Serratia marcescens* biofilms and plankton cells in microbial electrosynthesis systems. Sci Total Environ 666 (2019) 114-125. https://doi.org/10.1016/j.scitotenv.2019.02.267

Song X, Huang L, Lu H, Zhou P, Wang M, Li N. An external magnetic field for efficient acetate production from inorganic carbon in *Serratia marcescens* catalyzed cathode of microbial electrosynthesis system. Biochem Eng J 155 (2020) 107467. https://doi.org/10.1016/j.bej.2019.107467

Sun S, Huang L, Song X, Zhou P. An external magnetic field moderating Cr(VI) stress for simultaneous enhanced acetate production and Cr(VI) removal in microbial electrosynthesis system. Environ Res 193 (2021) 110550. https://doi.org/10.1016/j.envres.2020.110550

Wang S, Huang L, Gan L, Quan X, Li N, Chen G, Lu L, Xing D, Yang F. Combined effects of enrichment procedure and non-fermentable or fermentable co-substrate on performance and bacterial community for pentachlorophenol degradation in microbial fuel cells. Bioresour Technol 120 (2012) 120-126. https://doi.org/10.1016/j.biortech.2012.06.022

Wang Q, Huang L, Yu H, Quan X, Li Y, Fan G, Li L. Assessment of five different cathode materials for Co(II) reduction with simultaneous hydrogen evolution in microbial electrolysis cells. Inter J Hydrogen Energy 40 (2015) 184-196. https://doi.org/10.1016/j.ijhydene.2014.11.014

Wu Y, Du Q, Wan Y, Zhao Q, Li N, Wang X. Autotrophic nitrate reduction to ammonium via reverse electron transfer in *Geobacter* dominated biofilm. Biosens Bioelectron 215 (2022) 114578. https://doi.org/10.1016/j.bios.2022.114578

Xafenias N, Zhang Y, Banks CJ. Enhanced performance of hexavalent chromium reducing cathodes in the presence of *Shewanella oneidensis* MR-1 and lactate. Environ Sci Technol 47 (2013) 4512-4520. https://doi.org/10.1021/es304606u

Kan J, Hsu L, Cheung ACM, Pirbazari M, Nealson KH. Current production by bacterial communities in microbial fuel cells enriched from wastewater sludge with different electron donors. Environ Sci Technol 45 (2011) 1139-1146. https://doi.org/10.1021/es102645v

Xiao Y, Zhang E, Zhang J, Dai Y, Yang Z, Christensen HEM, Ulstrup J, Zhao F. Extracellular polymeric substances are transient media for microbial extracellular electron transfer. Sci Adv 3 (2017) e1700623. https://doi.org/10.1126/sciadv.1700623

Xue H, Zhou P, Huang L, Quan X, Yuan J. Cathodic Cr(VI) reduction by electrochemically active bacteria sensed by fluorescent probe. Sensor Actuat B-Chem 243 (2017) 303-310. http://dx.doi.org/10.1016/j.snb.2016.11.154

Yang G, Huang L, You L, Zhuang L, Zhou S. Electrochemical and spectroscopic insights into the mechanisms of bidirectional microbe-electrode electron transfer in *Geobacter soli* biofilms. Electrochem Commun 77 (2017) 93-97. https://doi.org/10.1016/j.elecom.2017.03.004

Yi Y, Ting Z, Zang Y, Xie B, Liu H. Different mechanisms for riboflavin to improve the outward and inward extracellular electron transfer of *Shewanella loihica*. Electrochem Commun 124 (2021) 106966. https://doi.org/10.1016/j.elecom.2021.106966

Yu SS, Cheng L, Chen JJ, Li WW, Zhao F, Wang WL, Li DB, Zhang F, Yu HQ. Framework of cytochrome/vitamin B_2 linker/graphene for robust microbial electricity generation. ACS Appl Mater Interfaces 10 (2018) 35090-35098. https://doi.org/10.1021/acsami.8b10877

Yu H, Huang L, Zhang G, Zhou P. Physiological metabolism of electrochemically active bacteria directed by combined acetate and Cd(II) in single-chamber microbial electrolysis cells. J Hazard Mater 424 (2022) 127538. https://doi.org/10.1016/j.jhazmat.2021.127538

Zhao F, Slade RCT, Varcoe JR. Techniques for the study and development of microbial fuel cells: an electrochemical perspective. Chem Soc Rev 38 (2009) 1926-1939. https://doi.org/10.1039/b819866g

Zhao M, Bai X, Zhang Y, Yuan Y, Sun J. Enhanced photodegradation of antibiotics based on anoxygenic photosynthetic bacteria and bacterial metabolites: A sustainably green strategy for the removal of high-risk organics from secondary effluent. J Hazard Mater 430 (2022) 128350. https://doi.org/10.1016/j.jhazmat.2022.128350

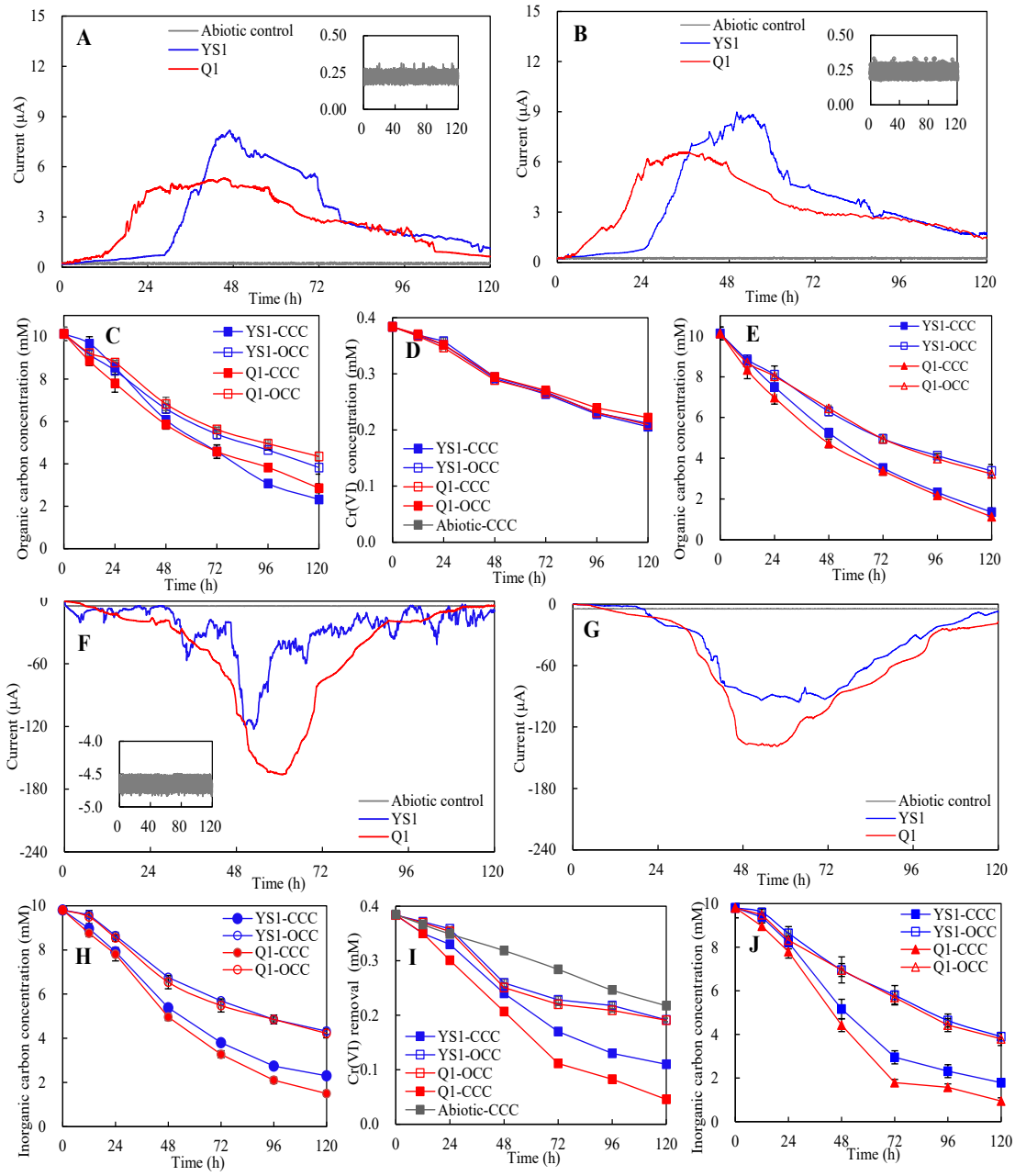

Figure 1 Electricity production (A, B, F and G), organic (C and E) or inorganic (H and J) carbons consumption, or Cr(VI) removal (D and I) by *Stenotrophomonas* sp. YS1 or *S. marcescens* Q1 as a function of operation time during outward (potential: +0.5 V vs. SHE) (A − E), or inward (potential: −0.5 V vs. SHE) (F − J) EET processes in the presence (A, C, D, F, H and I) or in the absence (B, E, G and J) of Cr(VI), or in the abiotic controls, or controls under open circuit conditions (OCCs).

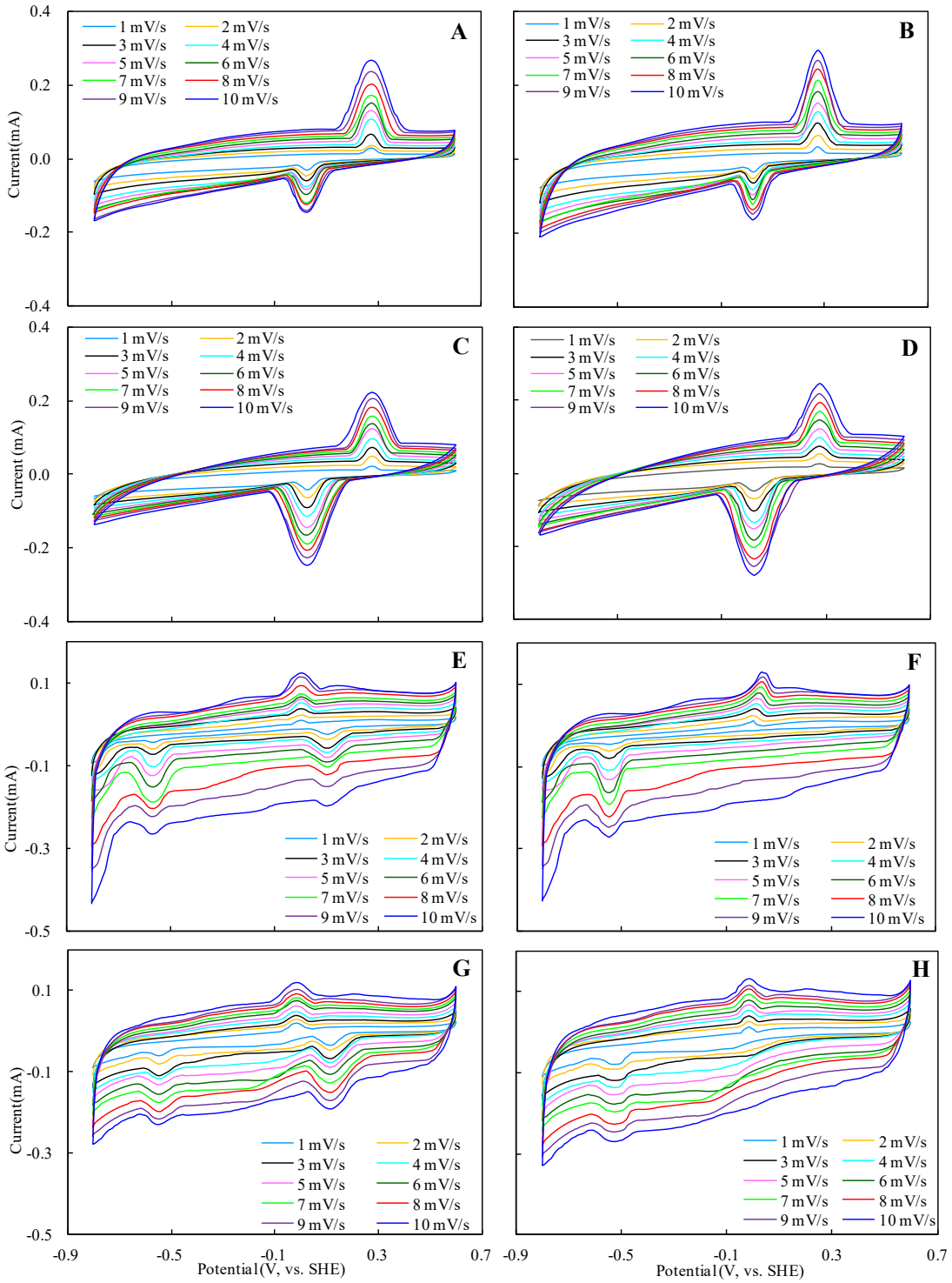

Figure 2 CV curves of *Stenotrophomonas* sp. YS1 (A, B, E and F) or *S. marcescens* Q1 (C, D, G and H) developed during outward (+0.5 V vs. SHE) (A − D) or inward (−0.5 V vs. SHE) (E − H) EET in the presence (A, C, E and G) or in the absence (B, D, F and H) of Cr(VI) at scan rates from 1 to 10 mV/s.

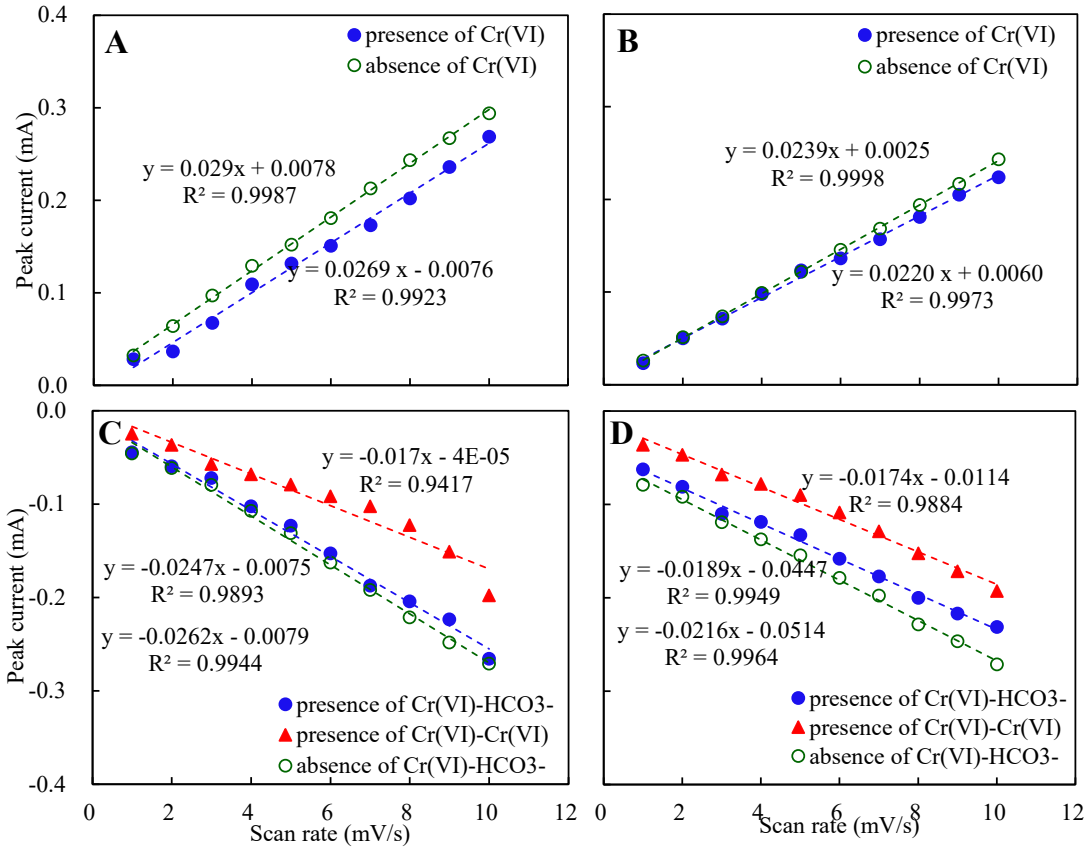

Figure 3 Correlations between the heights of the oxidation (A and B) or reduction (C and D) peaks and scan rates for *Stenotrophomonas* sp. YS1 (A and C) or *S. marcescens* Q1 (B and D) biofilms developed at +0.5 V vs. SHE (A and B) or −0.5 V vs. SHE (C and D) in the presence or in the absence of Cr(VI).

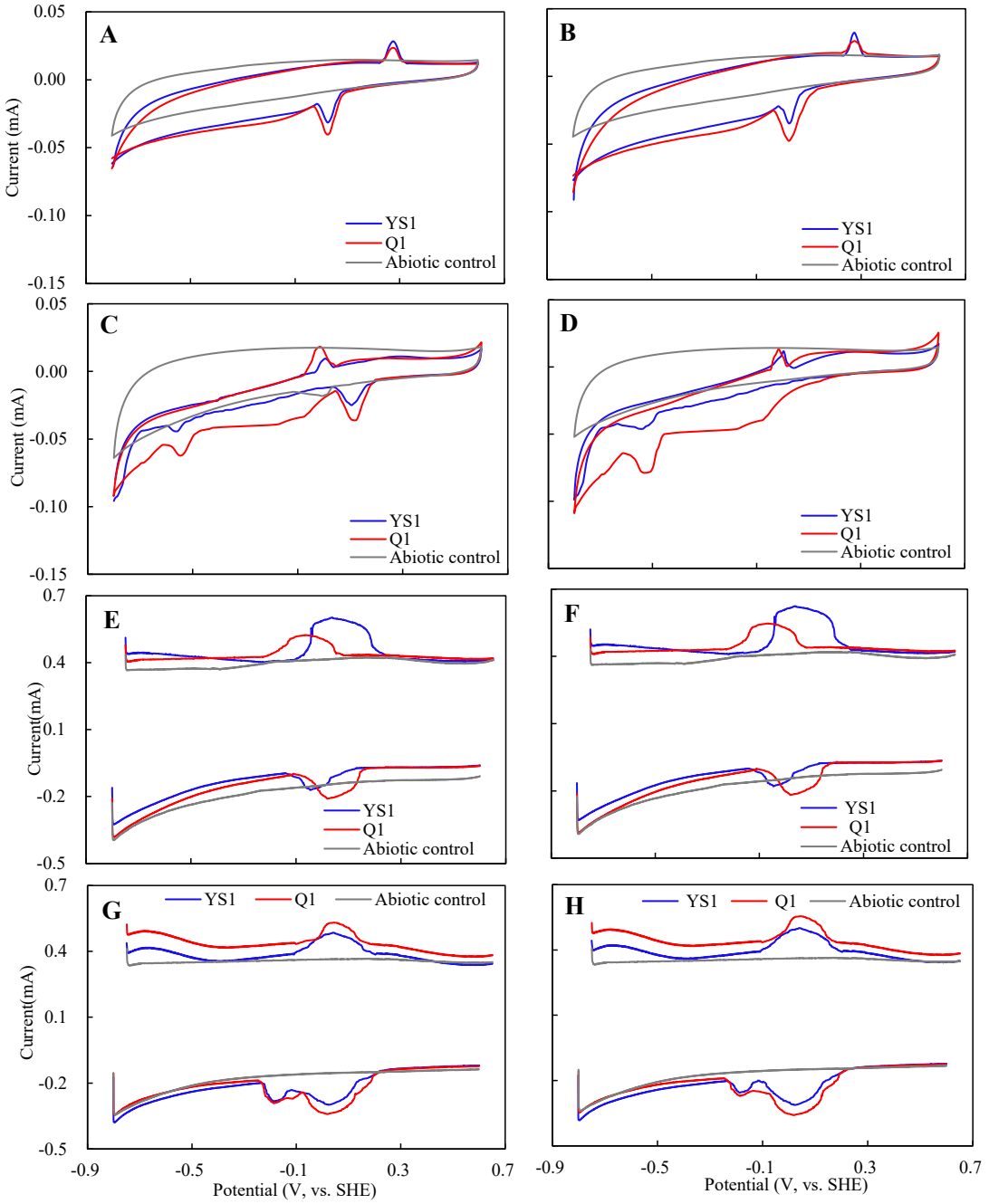

Figure 4 Comparison of CVs (A − D) or DPV (E − H) of *Stenotrophomonas* sp. YS1 and *S. marcescens* Q1 at either +0.5 V (A, B, E and F) or −0.5 V (C, D, G and H) in the presence (A, C, E and G) or in the absence (B, D, F and H) of Cr(VI) (scan rate: 1.0 mV/s).

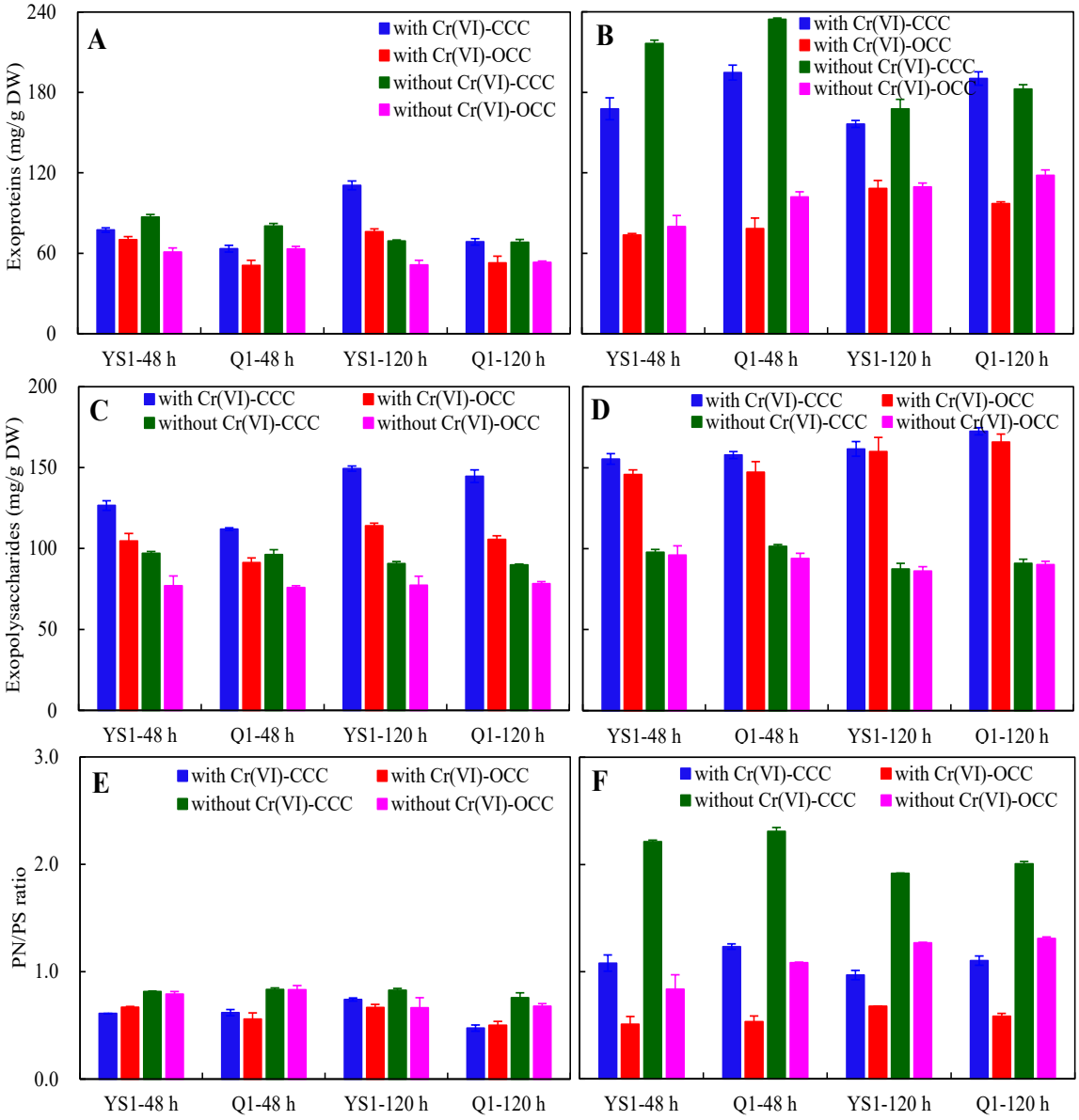

Figure 5 Exoproteins (A and B), exopolysaccharides (C and D), and ratios of exoproteins and exopolysaccharides (E and F), released by biofilms of *Stenotrophomonas* sp. YS1 or *S. marcescens* Q1 at either +0.5 V vs. SHE (A, C and E) or −0.5 V vs. SHE (B, D and F) and operational times of 48 h or 120 h in the presence or in the absence of Cr(VI) under closed circuit (CCC) or open circuit (OCC) conditions.

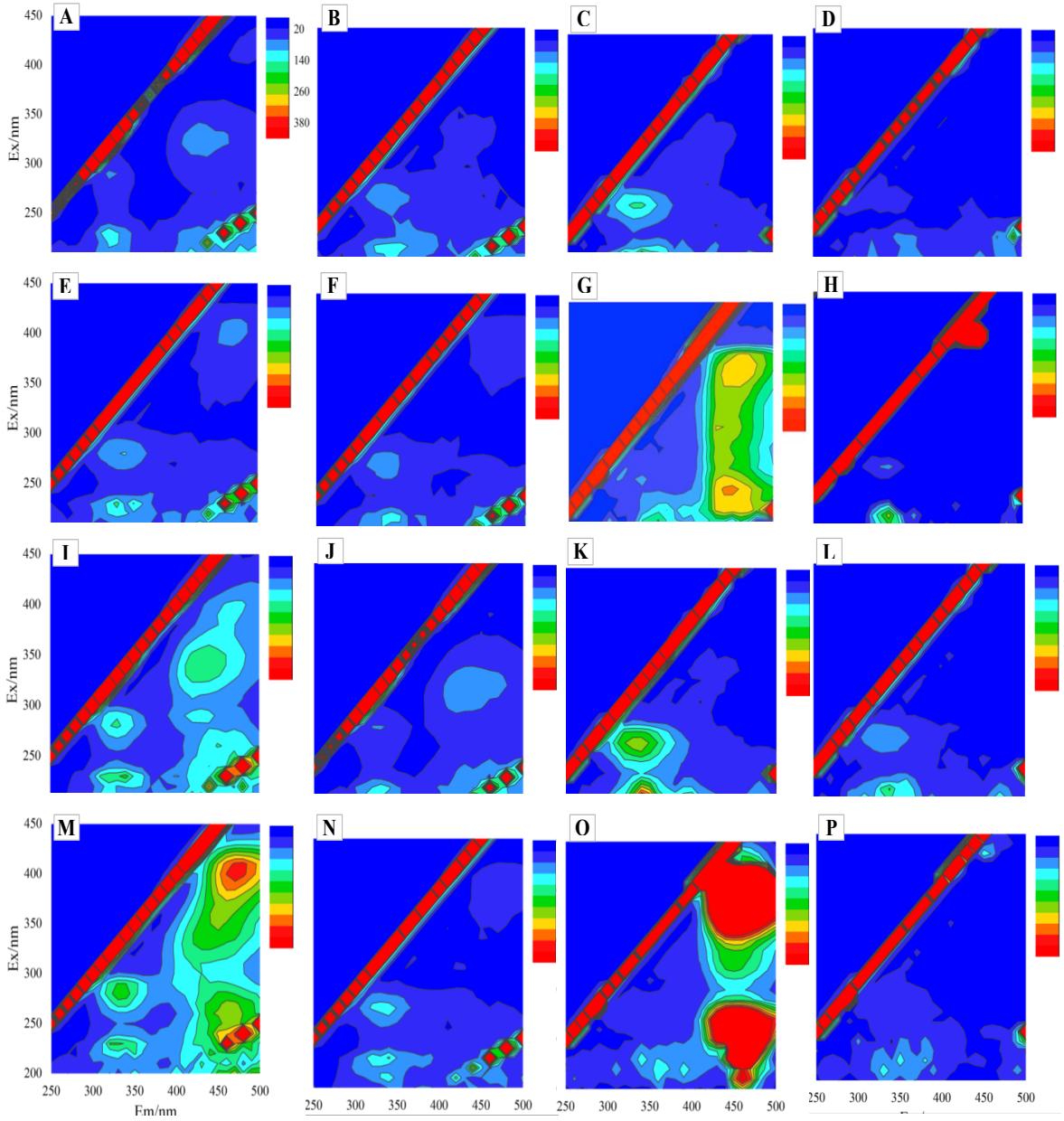

Figure 6 Fluorescence excitation emission matrix (FEEM) contours of extracellular polymer substances produced by biofilms of *Stenotrophomonas* sp. YS1 (A – D; I – L) or *S. marcescens* Q1 (E – H; M – P) at either +0.5 V vs. SHE (A − H) or −0.5 V vs. SHE (I − P) in the presence (A, B, E, F, I, J, M and N) or in the absence (C, D, G, H, K, L, O and P) of Cr(VI) under closed circuit (CCC) (A, C, E, G, I, K, M and O) or open circuit (OCC) (B, D, F, H, J, L, N and P) conditions (operation time: 48 h).

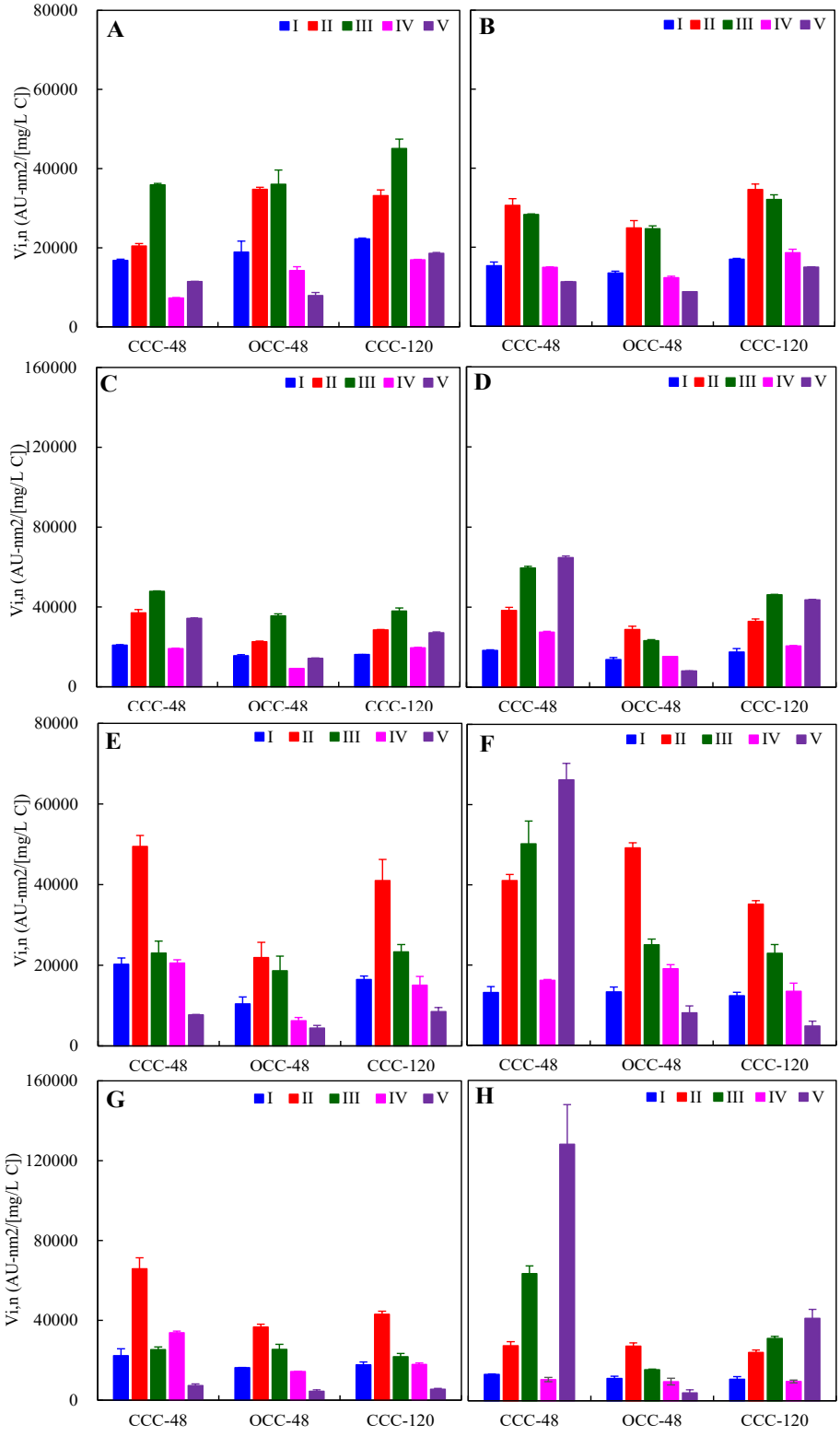

Figure 7 Absolute values of integral of fluorescence area of extracellular polymer substances produced by the biofilms of *Stenotrophomonas* sp. YS1 (A, C, E and G) or *S. marcescens* Q1 (B, D, F and H) at either +0.5 V (outward: A, B, E and F) or −0.5 V (inward: C, D, G and H) in the presence (A − D) or in the absence (E − H) of Cr(VI) at operational times of 48 h or 120 h under closed circuit (CCC) or open circuit (OCC) conditions.

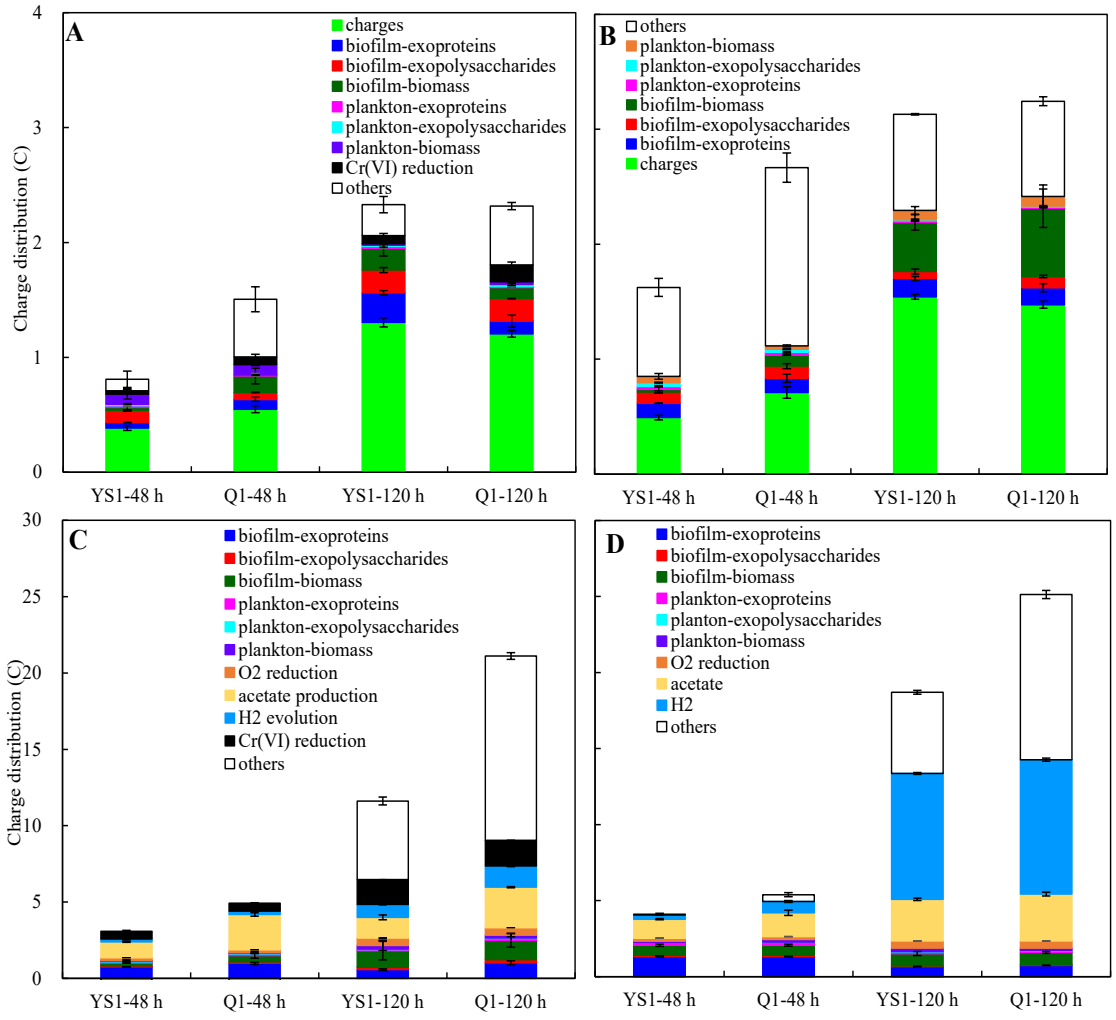

Figure 8 Charge distribution during outward (A and B) or inward (C and D) EET processes catalyzed by *Stenotrophomonas* sp. YS1 or *S. marcescens* Q1 at operational times of 48 h or 120 h in the presence (A and C) or in the absence (B and D) of Cr(VI).